

**Effect of inner structure of centrifugal separator  
on particle classification performance**

Tetsuya Yamamoto<sup>\*</sup>, Natsuko Watanabe, Kunihiro Fukui, Hideto Yoshida

Department of Chemical Engineering, Hiroshima University, 1-4-1, Kagamiyama,  
Higashi-Hiroshima 739-8527, Japan

Correspondence should be addressed to T. Yamamoto.

Phone: +81-824-24-7853

Fax: +81-824-24-5494

E-mail: [ytetsuya@hiroshima-u.ac.jp](mailto:ytetsuya@hiroshima-u.ac.jp)

## **Abstract**

This study investigated the effects of the inner structure of a centrifugal separator on particle classification performance. The typical inner structure of centrifugal separators is as follows: a blade, which consists of two orthogonal plates, is inserted into the centrifugal separator to create rigid fluid and particle rotations. The results of the present study demonstrate that centrifugal separator performance was significantly improved by attachment of a cylinder to the center of a conventional blade. Modification of the separator by attachment of the cylinder to the center of the centrifugal separator is expected to prevent the particles in the slurry from passing through the central axis of the centrifugal separator. Hence, the particles are subjected to greater centrifugal force. Both experimental and theoretical results demonstrate that particle classification performance increases **as the cylinder radius increases**. Thus, it is evident that attachment of a cylindrical blade to the center of the centrifugal separator allows for effective and highly efficient collection of extremely small-classified fine particles.

**Keywords:** Centrifugal separator; Classification; Cylinder; Particle size

## **1. Introduction**

Centrifugal separators can exert forces up to approximately 50,000 *g* on the fluid and particles that comprise liquid systems. Hence, centrifugal separators are widely used in the study of biology, minerals, and colloids for the removal of impurities from products in a short period of time. Recently, various industries, such as electronics, semiconductors, and medicine, have developed technologies that require monodispersed nanoparticles. Therefore, the development of a technique that classifies nanoparticles is extremely important. To date, classification techniques based on application of strong centrifugal forces have been developed for nanoparticles because conventional classification apparatus, such as cyclones and hydro-cyclones [1-7], are ineffective. In a recent study of centrifugal separators, we observed that dead space in the centrifugal separator decreased classification performance [8]. Furthermore, modification of the outlet structure to reduce the dead space enhanced classification performance [9].

In the present study, we focused on the effect of the inner structure of the centrifugal separator on its classification performance. We hypothesized that placement of a cylindrical blade at the center of the centrifugal separator would reduce the dead space and enhance classification performance.

## 2. Experimental procedure and theory

### 2.1. Centrifugal separator apparatus and experimental procedures

Figure 1 illustrates the centrifugal separator system used in the present study. The centrifugal separator is rotated at extremely high velocity by the motor attached to the top of the separator. The pump moves the original slurry from the slurry tank to the bottom of the centrifugal separator. The temperature and dispersion of which are controlled by a heater, stirrer, ultrasonic homogenizer (VC750, SONICS & MATERIALS, INC), and beads mill [10] (UAM-015, Kotobuki Industries Co.,LTD.). The particles in the slurry are subjected to a strong centrifugal force field, resulting in classification of the particles in the separator. The fine particles are collected from the top of the separator and the coarse particles remains in the separator. The conditions used in the present experimental system are listed in Table 1.

The dimensions of the centrifugal separator used in the present study are shown in Figure 2a. Figs. 2b and 2c show the details of both the conventional and cylindrical blades, which were inserted into the centrifugal separator to create rigid fluid and particles rotations. A disadvantage of the conventional blade is that particles near the central axis cannot be subjected to large centrifugal forces. As a result, even large particles cannot be collected at

the wall of the separator. In contrast, when a cylindrical blade is positioned at the center of the centrifugal separator, the cylinder prevents particles from passing through the central axis of the separator, thereby eliminating formation of dead space within the separator. It was expected that this modification of the inner structure of the centrifugal separator would improve classification performance.

Volumetric particle size distributions of the original and classified fine slurries were measured using dynamic light scattering (DLS, LB-550, HORIBA). Partial separation efficiency,  $\Delta\eta$ , defined by Eq.(1) was used to evaluate the classification performance of the centrifugal separator. Specially, the particle size on the partial separation efficiency curve, where  $\Delta\eta$  is equal to 0.95 was defined as the 95 % cut size of the centrifugal separator,  $D_{pc}$ ,

95.

The time which it took for the slurry to move from the bottom to the top of the separator was measured with a stop-watch and defined as the residence time of the slurry in the separator.

$$\Delta \eta = \frac{m_o f_o(D_p) \Delta D_p - m_f f_f(D_p) \Delta D_p}{m_o f_o(D_p) \Delta D_p} \quad (1)$$

## 2.2. Theoretical model equation of cut size of centrifugal separator

Figure 3 shows a schematic representation of the model centrifugal separator used to derive the theoretical equation for cut size of the centrifugal separator,  $D_{pc}$ , in  $r$ - $z$  coordinates (Eq.(2)). The  $r$ -coordinate position of the particle nearest the center and the inner radius of the centrifugal separator are represented by  $r_1$  and  $r_2$ , respectively. The derivation of this equation has been described in detail elsewhere [8,11]. In Eq.(2), when  $\Delta\eta$  is equal to 0.95,  $D_{pc}$  corresponds to  $D_{pc, 95}$ .

$$D_{pc}^2 = -\frac{9\mu}{\tau\omega^2(\rho_p - \rho)} \ln \left[ 1 - \Delta\eta \left\{ 1 - \left( \frac{r_1}{r_2} \right)^2 \right\} \right] \quad (2)$$

## 3. Results and discussion

### 3.1. Classification performance of the improved centrifugal separator

First, to determine if dead space existed within the centrifugal separator, residence time in the centrifugal separator,  $\tau$ , was determined experimentally and by theoretical calculations. In the theoretical calculation of residence time, the volume of the separator is divided by flow rate. As a result of positioning a cylindrical blade (radius =13 mm) at the center of the centrifugal separator, the experimentally determined residence time coincided

with the theoretically derived residence time. However, when residence time was evaluated when the conventional blade was used in the separator, the experimentally determined residence time was less than the calculated residence time. This result was attributed to generation of dead space within the separator. It is possible that the volume of the cylindrical blade compensates for the dead space in the separator.

Figure 4 illustrates the relationships between  $\tau$  and  $D_{pc, 95}$  for three blades. The dotted lines in Fig. 4 were drawn by fitting the experimental data to the equation for the theoretical model, in which  $r_1$  is regarded as the fitting parameter. Both the experimental and theoretical results demonstrate that increasing both the radius of the cylinder,  $r_c$ , and  $r_1$  lowers  $D_{pc, 95}$ . In other words, use of cylindrical blades effectively reduces  $D_{pc, 95}$ . In this way, we could explain our experimental results using the simple model equation, however, to fit the experimental results with theory and calculation more precisely, the numerical simulation considering the diffusion effect of particles, etc will be needed.

Under ideal experimental conditions,  $r_1$ , which is fitted, should approach  $r_c$  because particles cannot enter the cylinder. However, differences between  $r_c$  and  $r_1$  were observed in the present study. Error of the DLS measurement was investigated as an explanation for the differences. Particle size distributions measured using DLS and transmission electron

microscopy (TEM) are shown in Figure 5a. Particle size distribution was determined using TEM by measuring the diameter of 60,166 sample particles in the TEM images, as shown in Fig. 5b. Volumetric particle size distribution was then calculated. For particles less than 200 nm in diameter, peak size measured using DLS was greater than that measured by TEM. It is plausible that  $D_{pc, 95}$  (shown in Fig. 4) would give small-sized particles, because the size distribution determined experimentally using DLS measurement overestimates particle size. If particle size is accurately determined, then the value of the fitting parameter,  $r_1$ , will increase and approach the value of  $r_c$ .

### *3.2. Dependence of fine particle collection efficiency on $D_{pf, 95}$ of the fine slurry*

The collection efficiency of fine particles,  $y_f$ , is defined as the mass ratio of the collected classified fine particles,  $m_f$ , to the original particles,  $m_o$ . Figure 6 shows the relationship between  $y_f$  and the 95 % diameter of the cumulative distribution of fine particles,  $D_{pf, 95}$ , for various residence times. This result indicates that when  $D_{pf, 95}$  is greater than 0.25  $\mu\text{m}$ , the conventional blade effectively collects a large amount of fine particles from the top of the separator. However, for all other cases examined, the cylindrical blades were more effective than the conventional blade. The differences in effectiveness were

caused by differences in the relationship between collection efficiency and cumulative distribution (i.e., differences in slope of among the dotted lines determined by least squares fitting) among the blades. To examine the differences among blade type in greater detail, we partitioned the variation of  $y_f$  against  $D_{pf, 95}$ , into the variations of both  $y_f$  and  $D_{pf, 95}$  against  $\tau$ . As indicated in Figure 7, which shows the relationship between  $y_f$  and  $\tau$ ,  $y_f$  decreases as both the cylinder radius and residence time increase. These relationships are observed because the width of the fluid channel in the separator becomes so narrow that particles are subjected to greater centrifugal force and are readily deposited on the wall of the separator. However, the relationships between  $y_f$  and  $\tau$  described by least squares fitted lines were similar among the three blades. Hence, differences in slope of the dotted lines shown for the three blades in Fig. 6 were primarily attributed to variations in the relationship between  $D_{pf, 95}$  and  $\tau$ . As shown in Figure 8, the variation in  $D_{pf, 95}$  with  $\tau$  increased when the larger cylindrical blade was used. It is possible that the cylindrical blade reduces the sedimentation distance to the wall of the separator, so that residence time has a greater influence on  $D_{pf, 95}$ .

In summary, for a given  $D_{pf, 95}$ , the flow rate and residence time are unique to each blade. When  $D_{pf, 95}$  is extremely small, a cylindrical blade should be used for high

collection efficiency of the fine slurry. Thus, the technique of positioning a cylindrical blade at the center of the centrifugal separator is a useful method for highly efficient collection of nanoparticles.

### *3.3. Dependence of coarse particle collection efficiency on median particle size of the original slurry*

The relationships between  $D_{pc, 95}$  and  $\tau$ , and between  $y_f$  and properties of the classified fine slurry, such as  $D_{pf, 95}$ , described above pertain to the original slurry that was exposed only to ultrasonic homogenization under the conditions described in Table 1. In this section, we examine the dependence of  $y_f$  on the properties of the original slurry, such as median particle size,  $D_{p50}$ . To prepare original slurries with various median sizes, several dispersion methods, such as treatment with a beads mill, were used, as shown in Table 1. The resulting particle size distributions are shown in Figure 9. The smallest median particle size was obtained for the original slurry after 40 minutes of beads mill treatment. After separation of the various slurries, collection efficiency of coarse particles,  $1 - y_f$ , was measured for each slurry. The relationship between  $1 - y_f$  and  $D_{p50}$  at a residence time of  $\tau = 54$  s is shown in Figure 10. The cylindrical blade with a radius of  $r_c = 15$  mm was

effective for collection of the coarse particles, due to the shorter distance to the wall of the separator.

#### **4. Conclusions**

In conclusion, modification of the inner structure of the centrifugal separator by use of a cylindrical blade enhanced particle classification performance as follows:

- (1) The cylindrical blade **reduces** formation of dead space in the centrifugal separator and improves classification performance. In addition, use of a cylindrical blade with a larger radius reduces the 95 % cut size of the centrifugal separator.
- (2) The cylindrical blade is effective for highly efficient collection of fine particles.
- (3) The cylindrical blade effectively removes coarse particles from the original slurry.

#### **Acknowledgments**

This study was supported in part by The Information Center of Particle Technology, Japan.

## Nomenclature

$D_p$	particle diameter	( $\mu\text{m}$ )
$D_{pc}$	cut size of the centrifugal separator	( $\mu\text{m}$ )
$D_{pc, 95}$	95 % cut size of the centrifugal separator	( $\mu\text{m}$ )
$D_{pf, 95}$	95 % diameter of the cumulative distribution of fine particles	( $\mu\text{m}$ )
$\Delta D_p$	small difference of particle diameter	( $\mu\text{m}$ )
$f_o(D_p), f_f(D_p)$	particle size distributions of the original and classified fine particles, respectively	(-/ $\mu\text{m}$ )
$g$	acceleration due to gravity	( $\text{m/s}^2$ )
$m_o, m_f$	mass of the collected original and classified fine particles, respectively	(g/s)
$Q$	inlet flow rate	(mL/min)
$r_c$	radius of cylinder	(mm)
$r_1$	$r$ -coordinate position of particle nearest the center of the centrifugal separator	(mm)
$r_2$	inside radius of the centrifugal separator	(mm)
$y_f$	collection efficiency of fine particles	(-)

$\Delta \eta$	partial separation efficiency	(-)
$\mu$	fluid viscosity	(Pa·s)
$\rho, \rho_p$	fluid and particle density	(kg/m <sup>3</sup> )
$\tau$	residence time	(s)
$\omega$	rotational speed of centrifugal separator	(rpm)

## References

- 1 O. Molerus, M. Gluckler, Development of a cyclone separator with new design, Powder Technol. 86 (1996) 37–40.
- 2 H. Yoshida, K. Fukui, Y. Isshiki, Control of Particle Size Separation by Use of Hydrocyclone, J. Soc. Powder Technol., Japan 34(1997) 690–696.
- 3 H. Yoshida, K. Fukui, K. Yoshida, E. Shinoda, Particle separation by Iinoya's type gas cyclone, Powder Technol. 118 (2001) 16–23.
- 4 H. Yoshida, S. Akiyama, K. Fukui, A. Kumagaya, Particle Classification with Improved Hydro-cyclone Separator, J. Soc. Powder Technol., Japan 38(2001) 626–632.
- 5 Y. Norimoto, K. Fukui, H. Yoshida, Particle Classification Performance of Hydro-cyclone with Forced-vortex Type, J. Soc. Powder Technol., Japan 43(2006) 666–675.
- 6 H. Yoshida, K. Fukui, T. Yamamoto, A. Hashida, N. Michitani, Continuous Fine Particle Classification by Water-Elutriator with Applied Electro-potential, J. Soc. Powder Technol., Japan 43(2006) 550–558.
- 7 H. Yoshida, U. Norimoto, K. Fukui, Effect of blade rotation on particle classification

- performance of hydro-cyclones, Powder Technol., 164(2006) 103–110.
- 8 T. Yamamoto, T. Shinya, K. Fukui, H. Yoshida, Centrifugal Classification of Particles and Analysis of the Fluid Dynamics, J. Soc. Powder Technol., Japan 44(2007) 345–352.
  - 9 T. Yamamoto, T. Kotani, K. Fukui, H. Yoshida, Experimental and Computational Study of Classification of Particles by Improved Centrifugal Separator, J. Soc. Powder Technol., Japan 44(2007) 861–867.
  - 10 M. Inkyo, T. Tahara, T. Iwaki, F. Iskandar, C. J. Hogan, K. Okuyama, Experimental investigation of nanoparticle dispersion by beads milling with centrifugal bead separation, J. Colloid and Interface Sci., 304(2006) 535–540.
  - 11 H. Masuda, K. Higashitani, H. Yoshida, Powder Technology Handbook 3<sup>rd</sup> edition, CRC PRESS 2006, pp.545.

## FIGURES CAPTION

**Figure 1.** Experimental centrifugal separator system.

**Figure 2.** Details of: (a) the centrifugal separator; (b) the conventional blade; (c) the cylindrical blade.

**Figure 3.** Schematic representation of the theoretical model of the centrifugal separator in  $r$ - $z$  coordinates.

**Figure 4.** Relationships between residence time,  $\tau$ , and 95 % cut size,  $D_{pc, 95}$ , for the three blades.

**Figure 5.** Comparison of particle size distributions measured using DLS and TEM: (a) particle size distributions measured by DLS and TEM, (b) the corresponding TEM image of the particles.

**Figure 6.** Relationship between collection efficiency of fine particle,  $y_f$ , and 95 % diameter of cumulative distribution of the fine particles,  $D_{pf, 95}$ .

**Figure 7.** Relationship between collection efficiency of fine particle,  $y_f$ , and residence time,  $\tau$ .

**Figure 8.** Relationship between 95 % diameter of cumulative distribution of the fine

particles,  $D_{pf, 95}$ , and residence time,  $\tau$ .

**Figure 9.** Particle size distributions of the original slurry after treatment with various dispersion procedures.

**Figure 10.** Relationship between  $y_f$  and median particle size of the original slurry,  $D_{p50}$ .

**Table 1** Conditions of each part in the present experimental system.

Slurry conditions	<b><u>Slurry tank</u></b> Tested powder      Silica ( $\rho_p = 2300 \text{ kg/m}^3$ ) Medium                Water Concentration        0.5 wt% Temperature          30 °C
Dispersion conditions	<b><u>Ultrasonic homogenizer</u></b> Output                100 kW Operation time        10 min  <b><u>Beads mill</u></b> Beads                 150 $\mu\text{m}$ glass beads Flow rate             200 mL/min Rotation speed        2890 rpm Operation time        10 ~ 40 min
Classification conditions	<b><u>Centrifugal separator</u></b> Flow rate             200 ~ 600 mL/min Rotation speed        20000 rpm

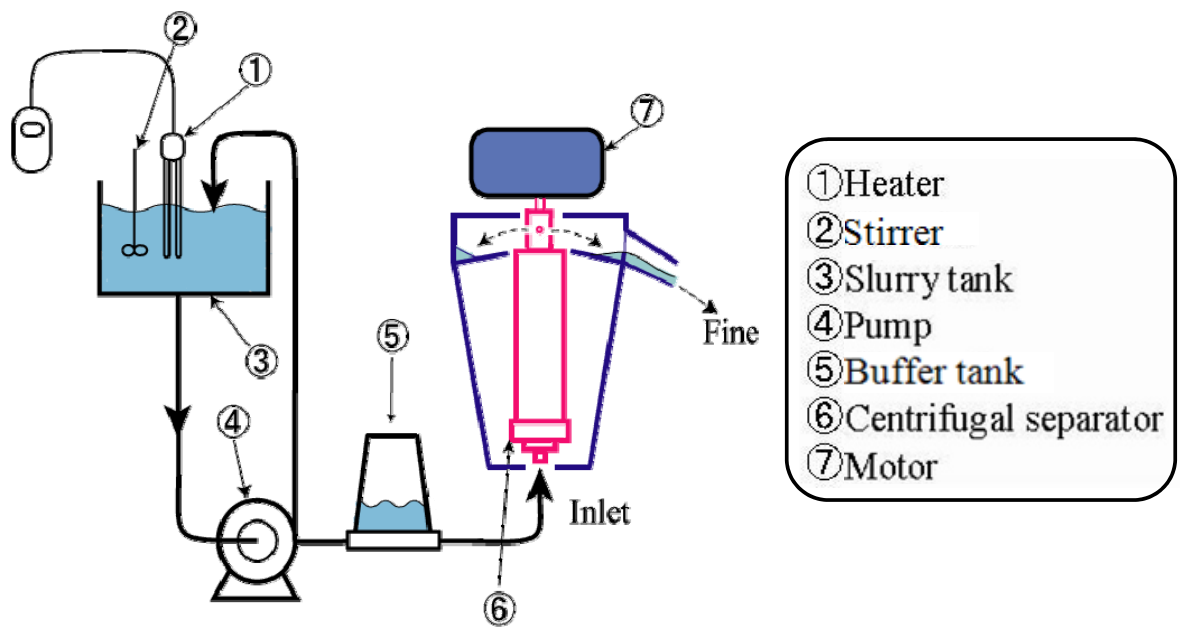


Figure 1

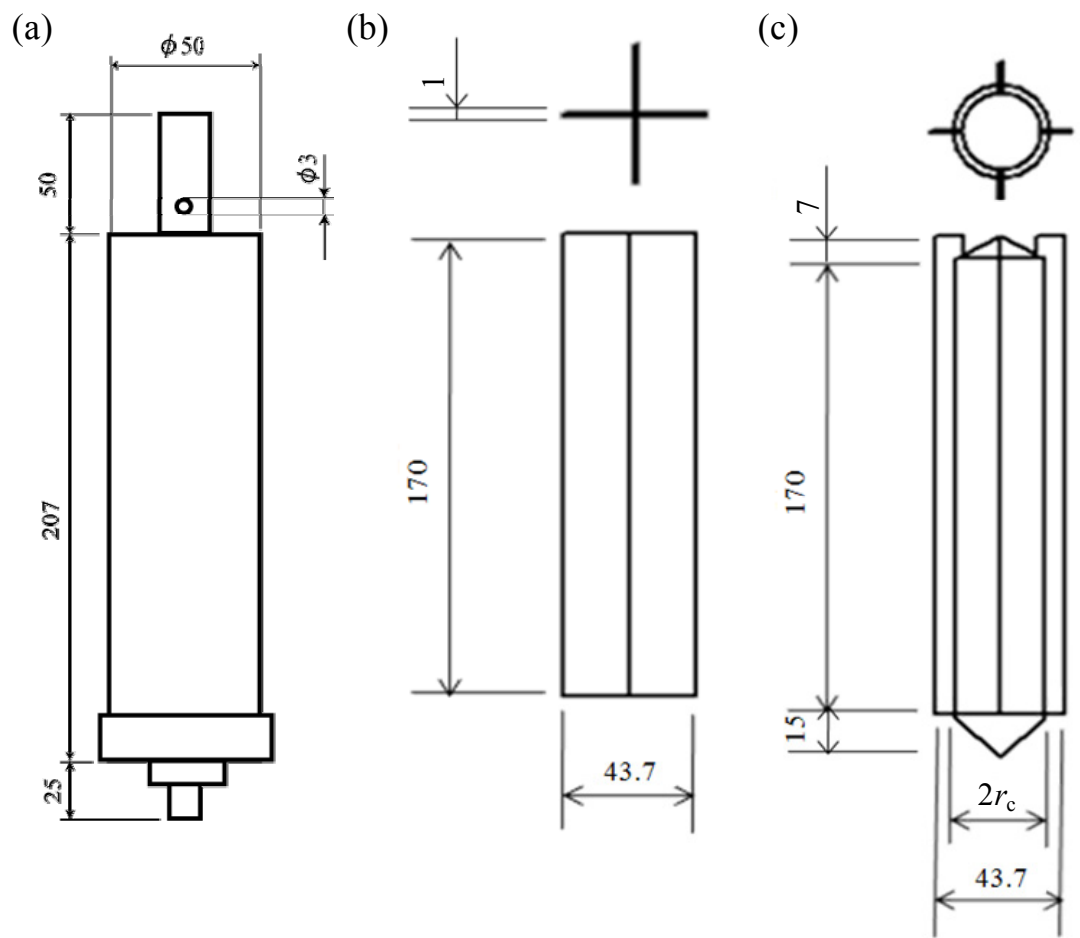


Figure 2

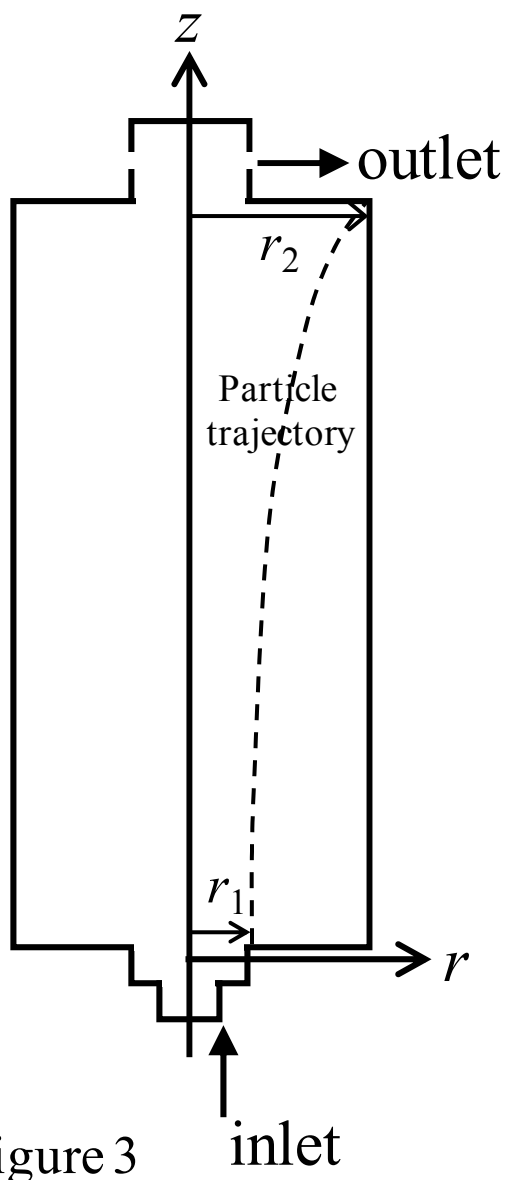


Figure 3

inlet

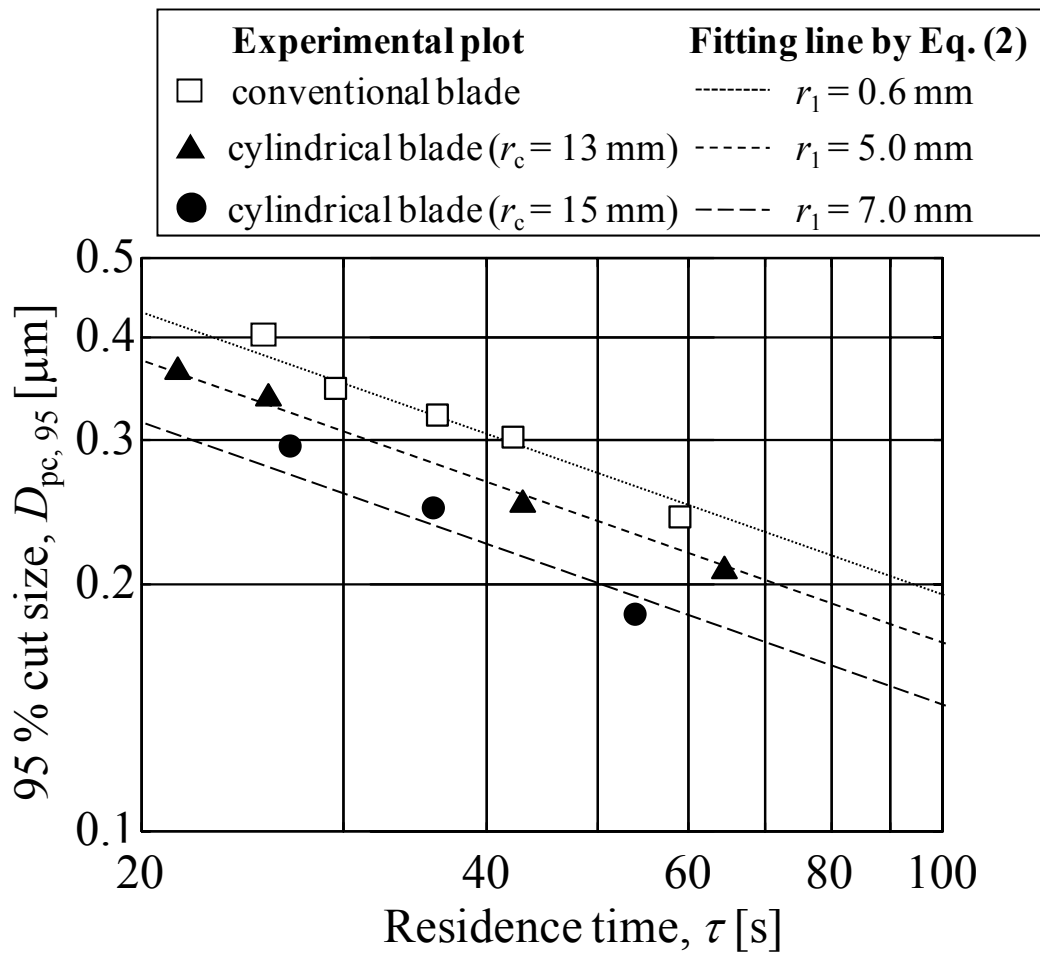


Figure 4

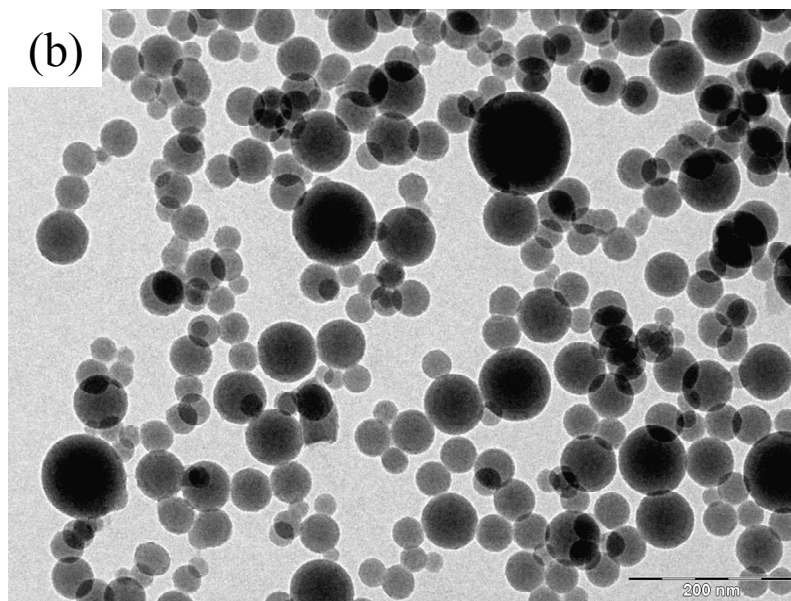
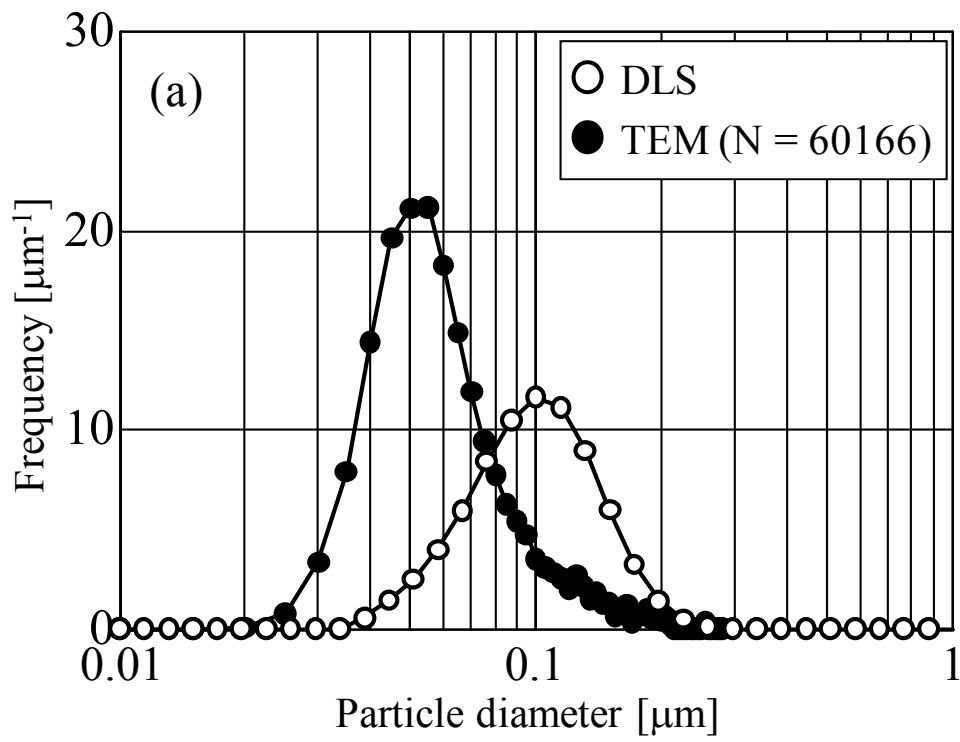


Figure 5

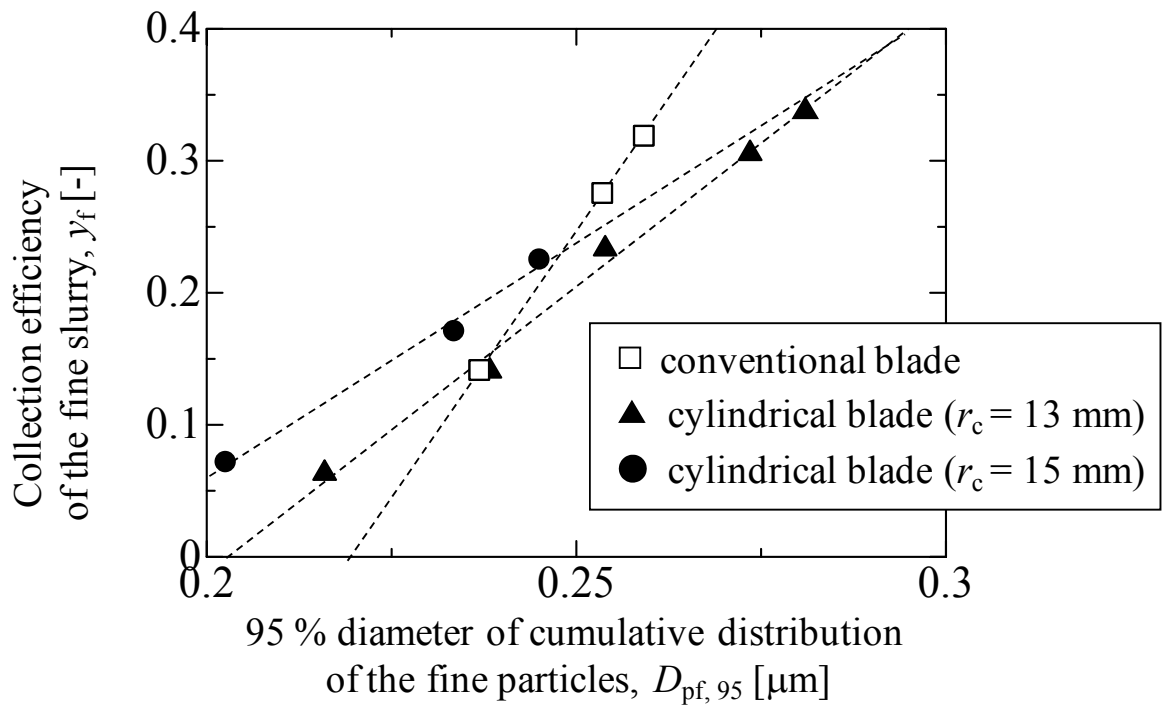


Figure 6

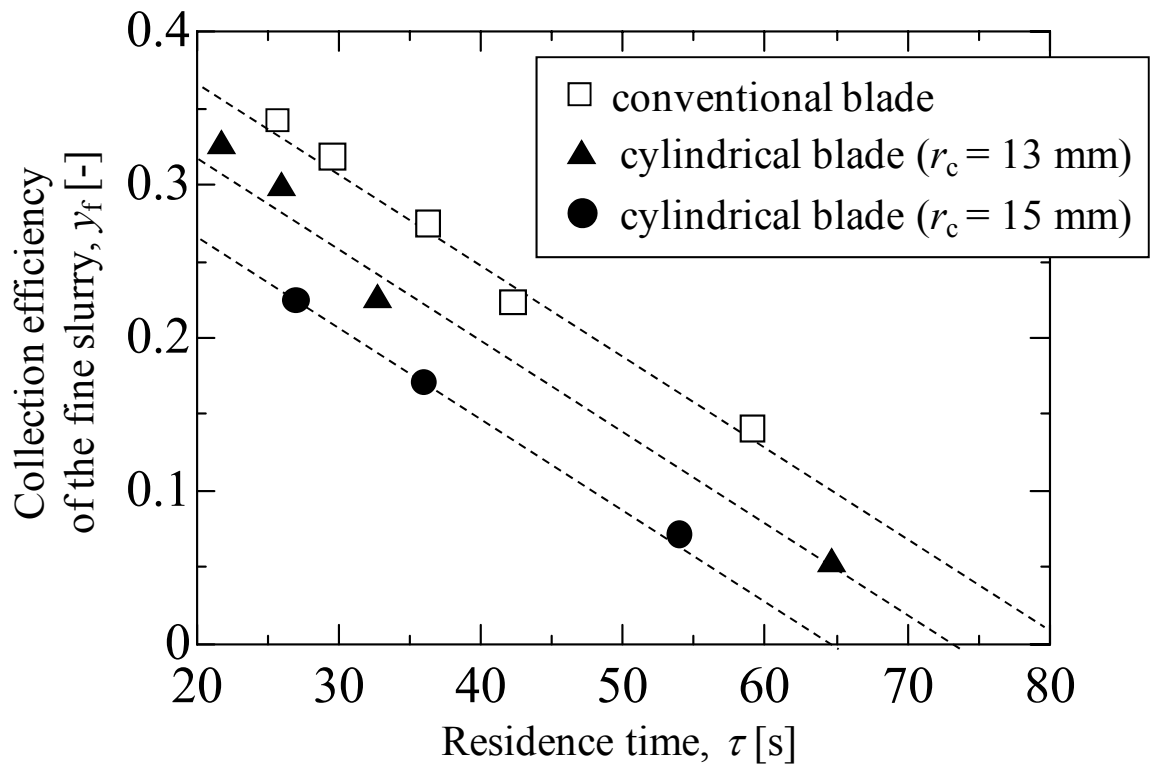


Figure 7

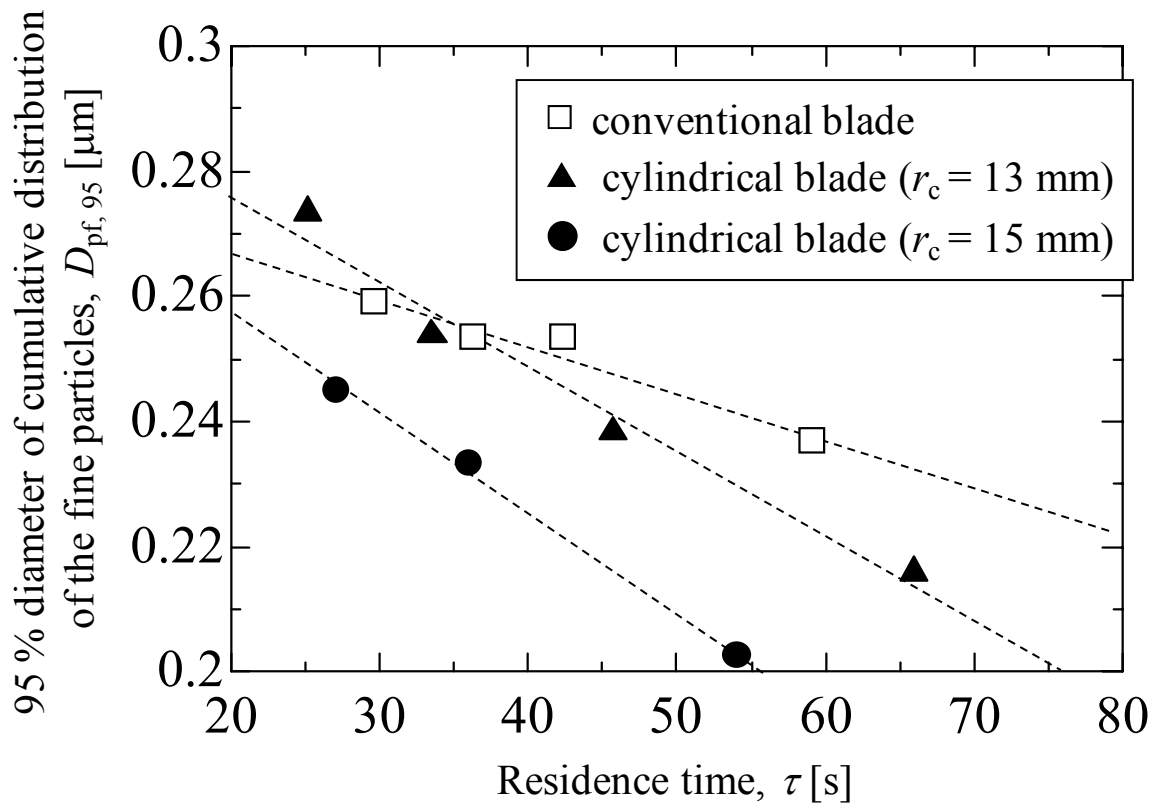


Figure 8

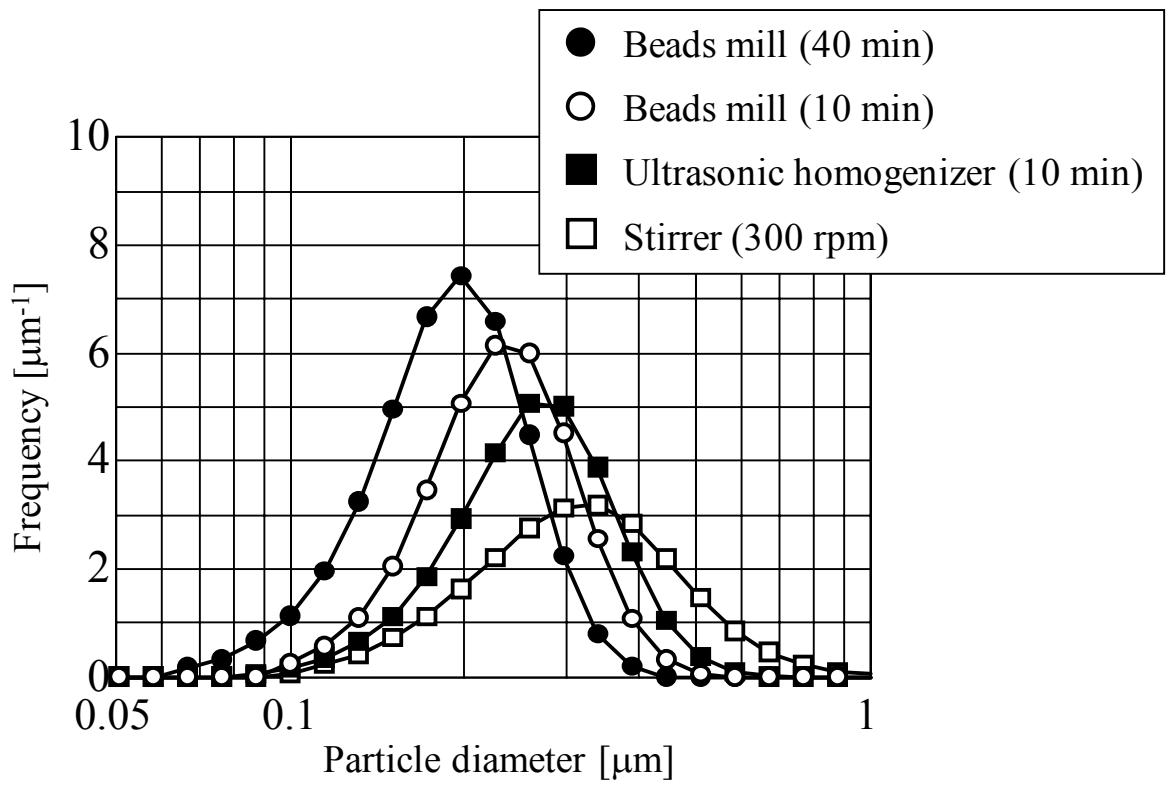


Figure 9

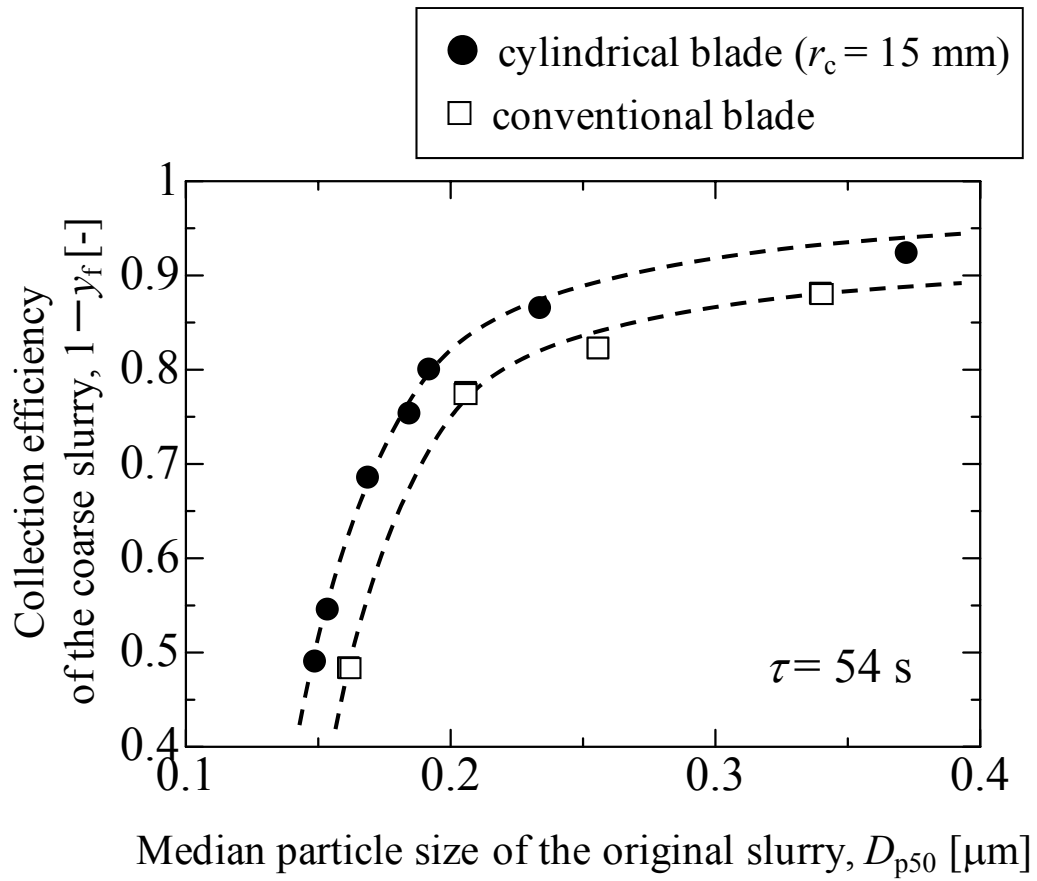


Figure 10